Original Research Article

MAGNETOHYDRODYNAMIC JEFFREY NANOFLUID FLOW OVER A VERTICAL SHEET

ABSTRACT

Aim

This focus on the numerical analysis of Jeffrey nano-fluid bound with magnetic field in presence of convectively heated boundary.

Study Design

Abstract, introduction, Equations formulation, numerical analysis and conclusion

Place and Duration of Study

Department of Mathematics and Actuarial Science, Kenyatta University, between 2021-2022

Methodology

This paper discusses the imposed magnetic field on Jeffrey fluid suspended with nanometre-sized particles moving over a vertical sheet with a convectively heated boundary. The partial differential equations are formulated by considering assumptions and the boundary conditions to describe the continuity, momentum, energy and concentration of the fluid. The similarity transformation technique was applied to convert the partial differential equations into first-order linear differential equations which were simulated in Matlab by invoking the Adam's-Moulton predictor-corrector scheme in ode113. The graphs have been analysed considering the effects of Deborah, Dufour-Lewis, Hartman, and Prandtl numbers respectively, solutal stratification, diffusion, thermophoresis, temperature grasshoff, mass grasshoff, relaxation-retardation parameters on the flow velocity, concentration, temperature, skin friction, heat and mass transfers are looked into.

Results

While Deborah number increased velocity, it reduced concentration, skin friction and thermal boundary layer at lower numbers hence improved mass and heat transfer. Solutal stratitication, Retardation-relaxation parameter and diffusion raised temperature thus heat transfer.

Conclusion

Deborah number, solutal stratification, retardation-relaxation parameter and diffusion improves heat and mass transfer.

Keywords [base fluid, Nanofluid, magneto-hydrodynamic, Brownian diffusion, Thermophoresis]

1. INTRODUCTION

Nanofluid is a uniform suspension of nanometre-sized metal particles in a base fluid. Metal microparticles of a diameter between 1-100nm are commonly used. Nanoparticles can be obtained from metals, oxides, carbon, nanotube and carbides. Base fluids include water, ethylene, oil, glycol, paraffine and ethanol while metals include Copper, aluminium, gold, and mercury. Nanofluid has better heat conductivity than the base fluid. Nanofluids are used to eject heat from nuclear reactors, cancer therapeutics, sensory and imaging, in nano dry delivery, as coolants in electronic components, nuclear reactors, heat exchangers

and in solar generation systems due to the enhanced thermal conductivity properties of nanofluids for heat transfer. The concentration, size and material of the nanoparticle determine thermal conductivity.

[1] studied the flow and heat transfer of magnetohydrodynamic Jeffrey nanofluid induced by a passively moving plate and numerically examined it. The findings, physical parameters over temperature profiles, Using the Runge Kutta Fehlberg method agreed with the previous model.

[2] Discussed the mixed convective flow of Jeffrey fluid near the axisymmetric stagnation point over an inclined permeable stretching cylinder where the results showed that temperature is a decreasing function of the thermal stratification parameter.

[3] Analyzed the nonlinear fractionalized Jeffrey fluid with the novel approach of the Atangana Bleanu fractional model where the results showed that the fractional model provided more than a line as compared to the classical model.

[4] Studied attributes of the convective flow of Jeffrey nanofluid with a vertical stretching plane surface incorporating magnetic influence. Among other results, it was shown that velocity profile diminished with large Hartman numbers.

[5] Researched natural convection viscoelastic Jeffrey's nanofluid flow from a vertical permeable flat plate with heat generation, thermal radiation and chemical reaction. The findings depicted that Debora number and suction parameter had related effects on the velocity profile.

[6] Examined the influence of viscous dissipation and Brownian motion on Jeffrey nanofluid over an unsteady moving surface with thermophoresis and mixed convection where graphical outcomes indicated that augmentation buoyance ratio and thermophoresis parameter led to diminished velocity curves and increased temperature curve.

[7] Researched effects of Joule heating and viscous dissipation on magnetohydrodynamic boundary layer flow of Jeffrey fluid over a vertically stretching cylinder. A larger Schmidt number decreased the concentration profile while it increased with a larger thermophoresis parameter.

[8] Explored slip flow of Jeffrey nanofluid with activation energy and entropy generation application. The findings were that slipped phenomena decay velocity profile while temperature and concentration directly related with Brownian motion parameter and activation energy.

According to [9], in the research on the Atangana Baleanu fractional model for the flow of Jeffrey nanofluid with diffusion thermo-effects applied in engine oil, the efficiency of engine oil improved when silver nanoparticles were increased.

[10] On mixed convection flow of a nanofluid in a vertical channel with a hall and ion slip effect observed that velocity increased at the hot wall and decreased at the cold wall due to increasing Jeffrey parameter.

[11] Enquired mechanism of the nonlinear convective flow of Jeffrey nanofluid due to nonlinear radially stretching sheet with convective conditions and magnetic field and found out that Deborah number enhanced velocity profile while thermal radiation enhanced temperature and heat transfer.

[12] Discussed numerical simulation of magnetohydrodynamic Jeffrey nanofluid and heat transfer over a stretching sheet considering Joule heating and viscous dissipation and concludes that silver water nanofluids have less velocity, local Nusselt number and local skin frictions than those of the base fluid. An increase in Deborah's number increased skin friction and Nusselt number which decreased by increased magnetic parameter.

[13] In the enquiry of magneto, Jeffrey nanofluid biconvection over a rotating vertical cone due to gyrotactic microorganisms observed that biconvection Rayleigh number and Schmidt number shrank the magnitude of tangential velocity and augmented the reduced density of the motile microorganisms respectively.

[14] In the investigation of Darcy Forchheimer's relation in magnetohydrodynamic Jeffrey nanofluid flow over a stretching surface noted that inertia and porosity factors declined momentum boundary while it increased the concentration of nanoparticles. From the foregoing none has posted about magnetohydrodynamic Jeffrey nanofluid flow over a vertical sheet which this work discusses to establish its suit for effective heat transfer.

2. MATHEMATICAL FORMULATION

Navier stokes equation does not describe all the rheological properties of the fluids used in technology and industries. The preferred non-Newtonian fluids are classified as differential type and rate type. The rate type has relaxation and retardation time. Jeffrey fluid is one of the rate types possessing linear viscoelastic feature which is applied in the manufacture of polymers. (Shahzad et al., 2018) stated that the steady time-independent derivative model $\tau = -PI + \frac{\mu}{1+\lambda_1}\left[R_1 + \lambda_2\left(\frac{\partial R_1}{\partial t} + \nabla v\right)R_1\right]$ where P is the

pressure, τ the Cauchy stress tensor, R_1 Rivline -Ericken tensor stated as $R_1 = \nabla v + \nabla v^t$. If $\lambda_1 = \lambda_2$, this model reduces to Navier Stokes equation; the fluid becomes Newtonian. Retardation time explains to the Jeffrey temperature flux model while relaxation time describes the time of fluid restoration from the deformed position to the initial stable state. Assuming that two-dimensional flow is streamlined, incompressible and an electrically conducting Jeffery nanofluid over a vertical sheet with plate y=0 and the fluid is magneto-hydrodynamically time-independent. The x-axis is perpendicular to the vertical sheet. Below is a geometrical representation of the model.

2.1 Equations Governing the Fluid Flow

Buongiorno used Brownian diffusion and thermophoresis in absence of turbulent effect\external forces to derive the conservative equations. The formulation of continuity, momentum, energy and concentration equations regulates the aforementioned model.

$$\frac{\partial u}{\partial x} + \frac{\partial v}{\partial y} = 0 \qquad 2.1.0$$

$$u\frac{\partial u}{\partial x} + v\frac{\partial u}{\partial y} = \beta g(T - T_\infty) + g\beta^*(C - C_\infty) + \frac{\gamma}{1+\lambda_1}\left(\frac{\partial^2 u}{\partial y^2} + \lambda_2\left(u\frac{\partial^3 u}{\partial x\,\partial y^2} + \frac{\partial u}{\partial y}\frac{\partial^2 u}{\partial x \partial y} - \frac{\partial u}{\partial x}\frac{\partial^2 u}{\partial y^2} + v\frac{\partial^3 u}{\partial y^3}\right)\right) - \frac{\sigma B_0^2 u}{\rho} \qquad 2.1.1$$

$$u\frac{\partial T}{\partial x} + v\frac{\partial T}{\partial y} = \alpha\frac{\partial^2 T}{\partial y^2} + \frac{\sigma B_0^2 u^2}{\rho c_p} + \tau\left[D_B\frac{\partial T}{\partial y}\frac{\partial C}{\partial y} + \frac{D_f}{T_\infty}\left(\frac{\partial u}{\partial y}\right)^2\right] \qquad 2.1.2$$

$$u\frac{\partial C}{\partial x} + v\frac{\partial C}{\partial y} = D_B\frac{\partial^2 C}{\partial y^2} + \frac{D_T}{T_\infty}\frac{\partial^2 T}{\partial y^2} \qquad 2.1.3$$

Subject to the boundary conditions at the surface of the vertical sheet and the free streams of the above equations expressed as

$$\left.\begin{array}{c} u = 0, v = 0, T = T_\omega(x), -k_\omega\frac{\partial T}{\partial y} = h_\omega(T_\omega - T), C = C_w(x)\ at\ y = 0 \\ u \to 0, v \to 0, T \to T_\infty(x), C \to C_\infty(x),\ as\ y \to \infty \end{array}\right\} \qquad 2.1.4$$

where *u* and *v* are the velocity components along the x-axis and y-axes direction respectively, $\gamma = \frac{\mu}{\rho}$ is the kinematic viscosity, λ_1 the ratio of relaxation time, λ_2 retarding time, β is the thermal expansion

coefficient of the fluid, ρ is the fluid density, g is the acceleration due to gravity, β^* is the volumetric expansion coefficient of the fluid**,** T_w is the boundary temperature of the fluid, C_w is the particle volume fraction on the boundary of the magnetic field, D_B is the Brownian diffusion coefficient, U_∞ is the free stream velocity on the boundary, T_∞ temperature of the particle far away from the fluid, C_∞ is the particle volume fraction far away from the fluid, and B is the imposed magnetic field, D_T is the thermophoretic diffusion coefficient, C_p is specific heat at constant pressure, τ is the ratio of heat capacity, σ is the electrical conductivity and ∞ is the value far away from the surface.

The freestream velocity, stratified free stream, plate surface temperature, particle concentration and unsteady magnetic field parameters are described as

Where a, b, and c are positive constants representing the assisting flow.

2.2 Transformation of the nonlinear equations

The set of equations describing this flow is non-linear. To solve them, they were transformed into a set of ordinary differential equations by the similarity transformation method.

2.2.1 Similarity transformation

By introducing the similarity transformation variables

$$\eta = \left(\frac{a}{v}\right)^{\frac{1}{2}} y, \psi = (av)^{\frac{1}{2}} xf$$

the boundary conditions and the partial differential equations 2.1.0-2.1.4 are transformed to

$$u = u_w = ax, v = 0, T = T_w, C = C_w \ \ at\ y = 0$$

$$u = 0, T \to T_\infty, C \to C_\infty \quad as\ y \to \infty$$

The free stream and the stream functions variables in this work are related to velocity along the x and y axes respectively as

$$u = \frac{\partial \psi}{\partial y} \text{ and } v = -\frac{\partial \psi}{\partial x} \qquad 2.2.1.1$$

Substituting Eqn.2.2.1.1 into equation 2.1.0

$$\frac{\partial}{\partial x}\left(\frac{\partial \psi}{\partial y}\right)+\frac{\partial}{\partial y}\left(-\frac{\partial \psi}{\partial x}\right)=0$$

Partially differentiating the introduced similarity transformation variables and substituting the result into equations 2.2.1.1,2.1.1-2.1.3 yield

$$u=axf^{'},v=-(av)^{1/2}f$$

$$f^{'''}-(1+\beta_1)((f^{'})^2-ff^{''}+Ha^2f^{'}-Gr-Gr^*)-\beta_2\left((f^{''})^2+f^{iv}\right)=0 \quad 2.2.1.2$$

$$\theta f^{'}+f^{'}\alpha-\theta^{'}f-Ha^2Ec(f^{'})^2-\theta^{'}\phi^{'}N_b-N_t(\theta^{''})^2-\frac{\theta^{''}}{Pr}=0 \quad 2.2.1.3$$

$$\phi f^{'}+f^{'}-f\phi^{'}-Ld\theta^{'}\phi-\frac{\phi^{''}}{Ln}=0 \quad 2.2.1.4$$

bearing upon the boundary conditions

$$\left.\begin{array}{c} f=0,f^{'}=1,\theta^{'}=-Bi(1-\theta),\phi=1\ at\ \eta=0 \\ f^{'}=0,\theta=0,\phi=0\ at\ \eta=\infty \end{array}\right\} \quad 2.2.1.5$$

Where

$$N_t=\frac{\tau D_T b^2 x}{vT_\infty}\ ,\alpha=\frac{n}{m},N_b=\frac{\tau D_B m x}{v}\ ,Ec=\frac{a^2x}{C_p}\ ,\phi=\frac{C_w-C_\infty}{C_\infty}$$

$$Ha^2=\frac{\sigma B_0^2}{\rho a},Ld=\frac{D_T(T_\omega-T_\infty)bx}{vT_\infty},Ln=\frac{v}{D_B}\ ,G_r=\frac{g\beta(b-c)}{a^2},G_r^*=\frac{g\beta^*(m-n)}{a^2}$$

$$\beta_2=\lambda_2 a\ ,Pr=\frac{\alpha}{v},\beta_1=(1+\lambda_1)$$

are thermophoresis, solutal stratification and diffusion parameters, Eckert, Hartman, DuFour Lewis, Nano-Lewis, Temperature Grashoff, mass Grashoff, Deborah and Prandtl numbers respectively, β_1, a Jeffrey fluid parameter, θ temperature, ϕ concentration and f dimensionless stream function, η similarity variable and ψ the stream function.

The skin friction coefficient Cf_x , Heat transfer rate (Nusselt number) Nu_x and mass transfer rate (Local nano-Sherwood number) Sh_x prescribed as

$$Cf_x = \frac{\tau_\omega}{\rho(u_\omega^2)}\ , Nu_x = \frac{q_\omega}{k(T_\omega - T_\infty)}\ , Sh_x = \frac{q_m}{D_B(C_\omega - C_\infty)}$$

With the surface nano-shear stress τ_ω, surface nano heat flux q_ω and surface nano mass flux q_m expressed as

$$\tau_\omega = \mu\frac{\partial u}{\partial y}\ , q_\omega = -k\frac{\partial T}{\partial y}\ , q_m = D_B\frac{\partial C}{\partial y}$$

By appropriate substitution, the skin friction coefficient, Nusselt number and Sherwood numbers obtained are $Cf_x Re_x^{\frac{1}{2}} = f''\ , Nu_x Re_x^{-\frac{1}{2}} = -\theta'\ , Sh_x Re_x^{-\frac{1}{2}} = \phi'$ with

$Re_x = \frac{xa}{v}$ as the Local Reynolds number

3. NUMERICAL PROCEDURE

The linear-less boundary equations 2.2.1.2-2.2.1.4 subject to the boundary condition 2.2.1.5 are solved numerically using the Adams-Moulton predictor-corrector scheme by first converting to states variable form and invoking Matlab bvp5c function.

3.1. states variable form

$$x_1 = f, x_2 = f'\ , x_3 = f''\ , x_4 = f'''\ , x_5 = f^{iv}, x_6 = \theta, x_7 = \theta', x_8 = \theta''\ , x_9 = \phi, x_{10} = \phi'\ ,$$

$$x_{11} = \phi''$$

$$x_1' = x_2$$

$$x_2' = x_3$$

$$x_3' = x_4$$

$$x_4' = (1+\beta_1)(x_2^2 - x_1x_3 + Ha^2x_2 - Gr - Gr*) - \beta_2(x_3^2 + x_5)$$

$$y_5' = x_6$$

$$x_6^{'} = x_7$$

$$x_7^{'} = Pr[x_2 x_6 + x_1 \alpha - x x_7 + HaEc x_2^2 - x_7 x_{10} N_b - x_8^2 N_t]$$

$$x_8^{'} = x_9$$

$$x_9^{'} = x_{10}$$

$$x_{10}^{'} = Ln(x_9 x_2 + x_2 - x_1 x_{10} - x_7 x_{10} Ld)$$

Subject to the dimensionless boundary conditions

$$x_1 = 0, x_2 = 1, x_7 = -Bi(1 - x_6), x_9 = 1 \; at \; \eta = 0$$

$$x_2 = 0, x_6 = 0, x_9 = 0 \; at \; \eta = \infty$$

4. GRAPHICAL ANALYSIS

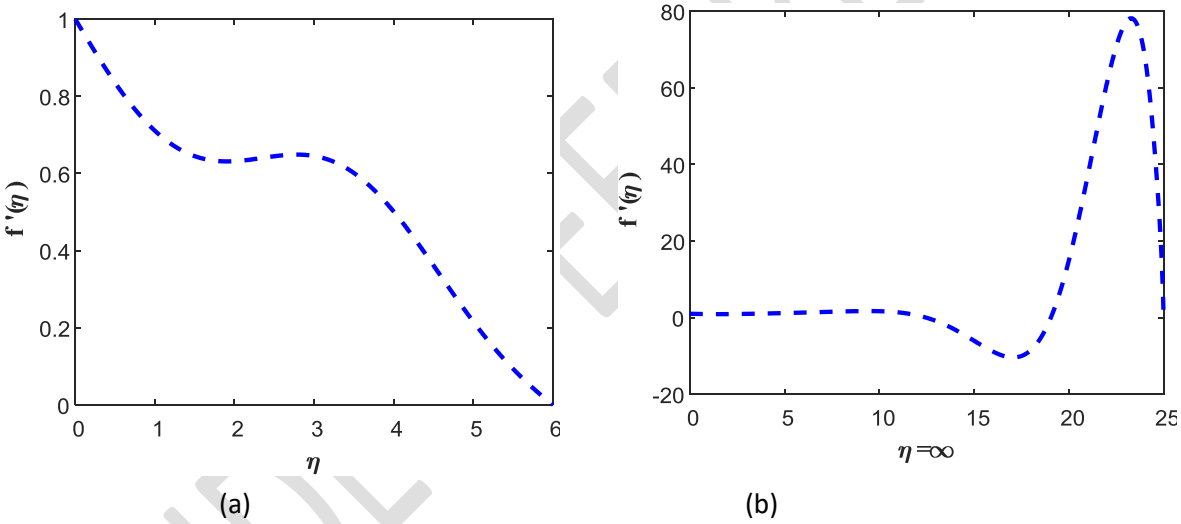

Fig. 1. (a) and (b) Boundary Conditions

This study looks into the effects of Hartman, Deborah, Prandtl, Mass Grassoff, temperature Grashoff, solutal stratification, relaxation-retardation, thermophoresis, diffusion, Dufour on velocity, temperature, concentration and the consequences to skin friction, Nusselt and Sherwood numbers in presence of convectively heated boundary from fig.1 to fig.30.

The graphs in Fig.1. (a) and (b) satisfy the boundary conditions of equation 2.1.4

4.1. Velocity profiles

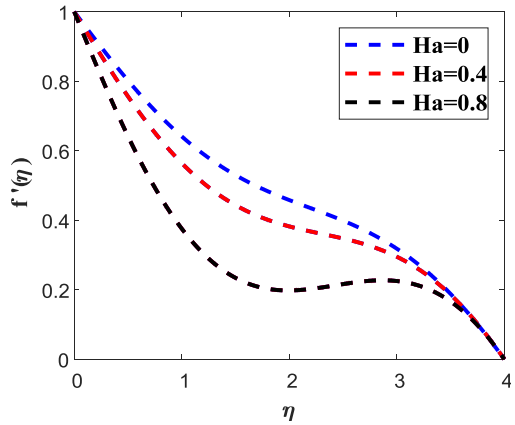

Fig.3. Effect of Hartman number
Pr=6.1,Ld=0.3,B=1,β_1 =0.1, ,β_2 =0.06,Gr=0.3, Gr=0.3,N_b=1.3,N_t=1.2,L=1.5,Ec=0.1,α=0.2*

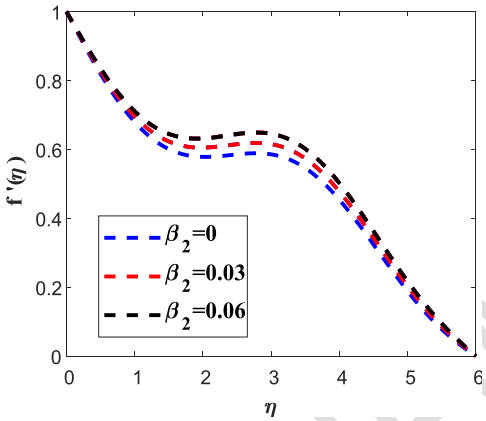

Fig.4. Effect of Deborah's number
Pr=6.1,Ld=0.3,B=1, β_1 =0.1,Gr=0.3,Gr=0.3, N_b=1.3,N_t=1.2,L=1.5,Ha=0.1,E=0.1, α =0.2*

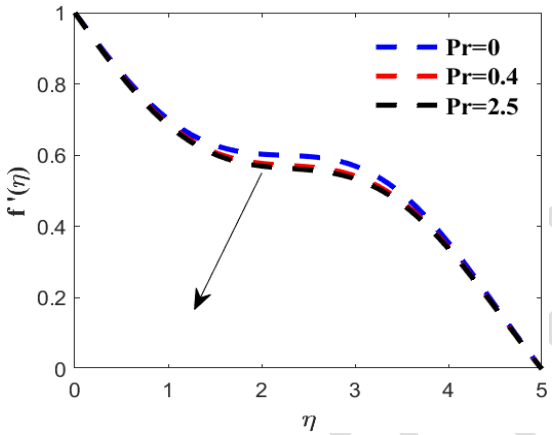

Fig.5. Effect of Prandtl number
Ld=0.3,B=1, β_1 =0.1, β_2 =0.06,Gr=0.3, Gr=0.3,N_b=1.3,N_t=1.2,L=1.5,Ha=0.1,Ec=0.1, α =0.2*

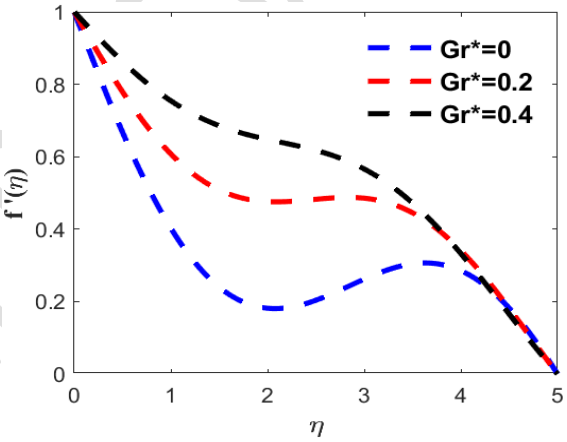

Fig.6. Effect of mass Grashoff
Pr=2.5,Ld=0.3,B=1, β_1 =0.1, β_2 =0.06,Gr=0.3, N_b=1.3,N_t=1.2,L=1.5,Ha=0.1,Ec=0.1, α =0.2

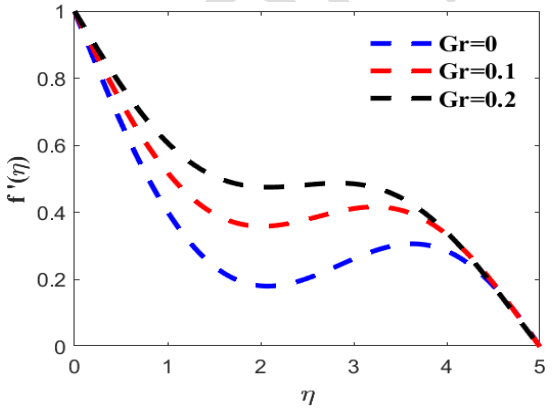

Fig. 7. Effect of mass temperature
Pr=2.5,Ld=0.3,B=1, β_1 =0.1, β_2 =0.06,Gr =0.3, N_b=1.3,N_t=1.2,L=1.5,Ha=0.1,Ec=0.1, α =0.2*

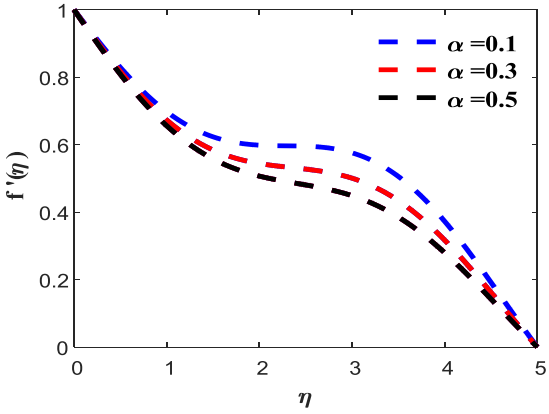

Fig. 8. Effect of solutal stratification
Pr=6.2,Ld=2.4,B=1, β_1 =0.1, β_2 =0.06, Gr=0.3,Gr=0.3,N_b=1.3,N_t=1.2,L=1.5,Ha=0.1,Ec=0.1*

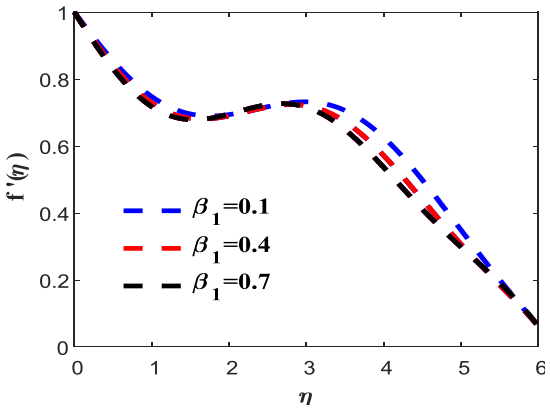

Fig.9. Effect of relaxation-retardation
Pr=6.2, Ld.=2.4, B=1, β_2 =0.06, Gr=0.3, Gr=0.3, N_b=1.3,N_t=1.2,L=1.5,Ha=0.1,Ec=0.1, α = 0.2*

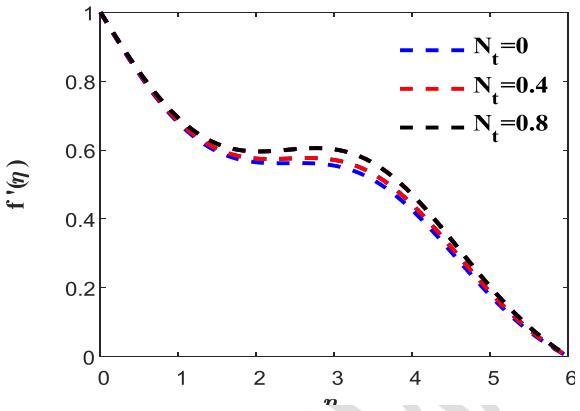

Fig.10. Effect of thermophoresis
Pr.=6.2, Ld.=2.4, B=1, β_1 =0.1, β_2 =0.06, Gr=0.3,Gr=0.3, N_b=1.3,L=1.5,Ha=0.1,E=0.1, α = 0.2*

Figs. 3,5,9 and 8 depict an increase in Hartman number, Prandtl number, Relaxation-Retardation and solutal stratification together with the similarity variable decreased velocity. The magnetic field interacts with the electrically conducting Jeffrey nanofluid to cause a Lorenz force which slows down velocity. The increase in Prandtl number increases thermal diffusivity and thermal boundary layer. This is due to the increased rate of Jeffrey nanoparticle fluid collisions, reduced buoyant force, heat dissipation and viscosity. The density of the nanofluid determines stratification. The layering has a similar effect. From figs. 4,6,7 and 10 show that an increase in Deborah number, Mass Grashoff, thermophoresis and mass temperatures leads to a corresponding increase in velocity; decreased resistance in the boundary layer caused by higher buoyant forces, temperature and migration of fresh mass particles.

4.2. Temperature profiles

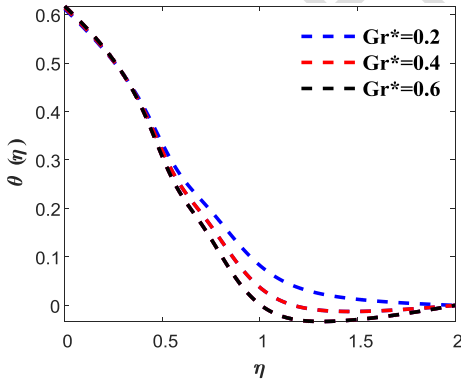

Fig.11.Effect of mass Grashoff
Pr=6.2, Ld=2.4, B=1, β_1 =0.1, β_2 =0.06, Gr=0.3, N_b=1.3,N_t=1.2,L=1.5,Ha=0.1,Ec=0.1, α = 0.2

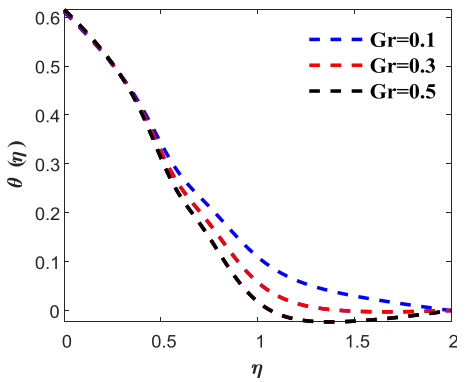

Fig.12. Effect of temperature Grashoff
Pr=6.2, Ld=2.4, B=1, β_1 = 0.1 β_2 =0.06,Gr=0.3, N_b=1.3,N_t=1.2,L=1.5,Ha=0.1,Ec=0.1, α = 0.2*

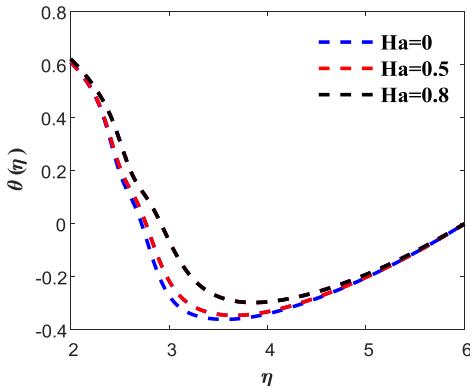

Fig.13. Effect of Hartman number
Pr=6.2, Ld=2.4, B=1, β_1 = 0.1, β_2 =0.06,Gr=0.3, N_b=1.3,N_t=1.2,L=1.5,Ec=0.1, α = 0.2*

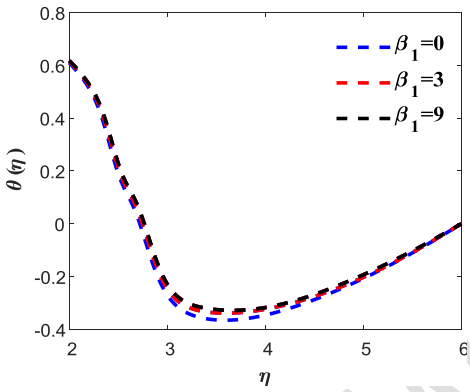

Fig.14. Effect of relaxation-retardation
Pr=6.2, Ld=2.4, B=1,β_2 =0.06, Gr=0.3, Gr=0.3,N_b=1.3,L=1.5,Ha=0.1,Ec=0.1, α = 0.2*

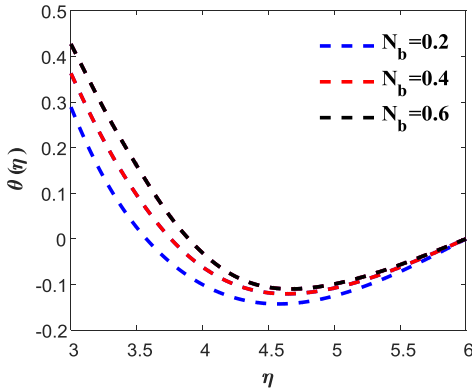

Fig.15. Effect of Diffusion
Pr=6.2, Ld=2.4, B=1, β_1 =0.3, β_2 =0.06, Gr=0.3, Gr=0.3,N_t=1.2,L=1.5,Ha=0.1,Ec=0.1, α =0.2*

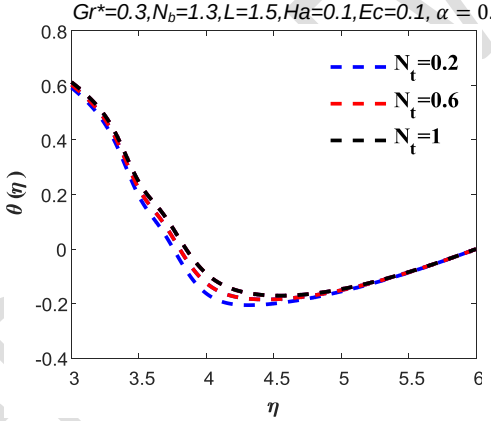

Fig.16.Effect of thermophoresis
Pr=6.2, Ld=2.4, B=1, β_1 =0.3, β_2=0.06, Gr=0.3, Gr=0.3,N_b=1.3,L=1.5,Ha=0.1,Ec=0.1, α =0.2*

Figs. 11 and 12 show that an increase in mass and temperature Grasshoff decreases temperature as a result of reduced viscosity and collision rate between the influx of fresh and heated particles. Figs.13-16 infer the growth of Hartman number, retardation-relaxation, diffusion and thermophoresis increase temperature. The viscosity of nano-particles and resistive force of the electromagnetic field hike temperature. Nano-particles distribute energy from convectively heated boundaries to other particles at a lower temperature.

4.3. Concentration profiles

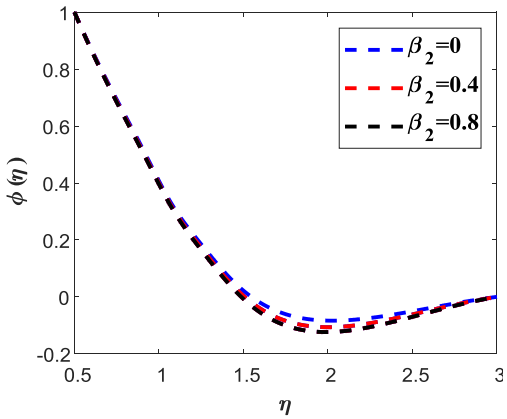

Fig.17. Effect of Deborah number

Pr=6.2, Ld=2.4, B=1, β_1 =0.3,Gr=0.3,Gr=0.3,N_b=1.3, N_t=1.2,L=1.5,Ha=0.1,Ec=0.1, α =0.2*

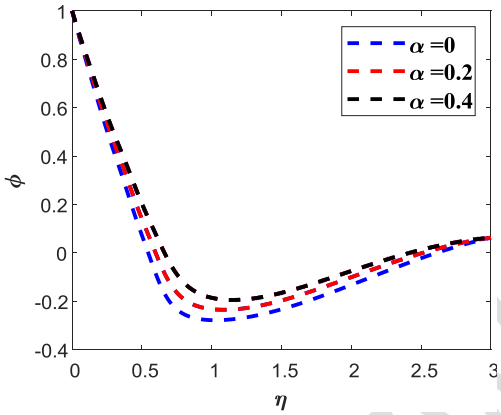

Fig.18. Effect of solutal stratification

Pr=6.2, Ld=2.4, B=1, β_1 =0.3 , β_2=0.4,Gr=0.3,Gr=0.3, N_b=1.3,L=1.5,Ha=0.1,Ec=0.1, α =0.2*

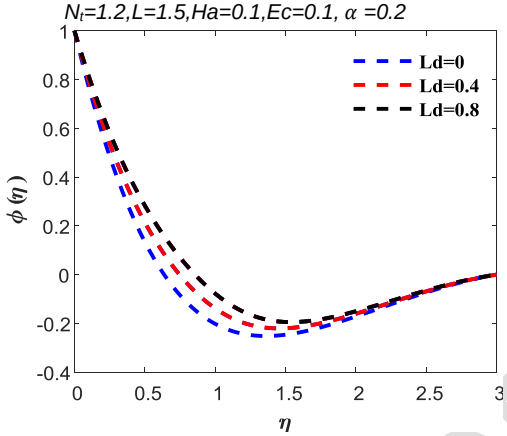

Fig.19. Effect of Dufour number

Pr=6.2, B=1, β_1 =0.3, β_2 =0.4, Gr=0.3,G=0.3,N_b=1.3, L=1.5,Ha=0.1,Ec=0.1, α =0.2,N_t=1.2

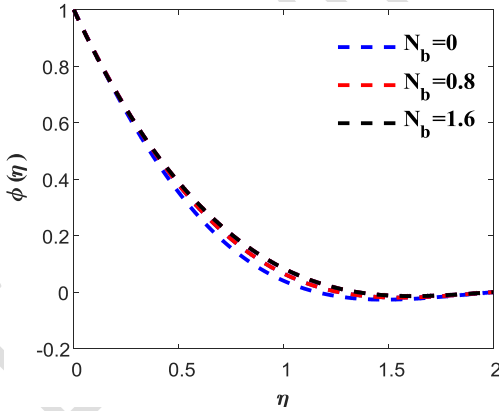

Fig.20.Effect of Diffusion

Pr=2,Ld=1.6,B=1, β_1 =0.3, β_2 =0.4,Gr=0.3,G=0.3, N_b=1.6,N_t=1.2,L=1.5,Ha=0.1,Ec=0.1, α =0.2

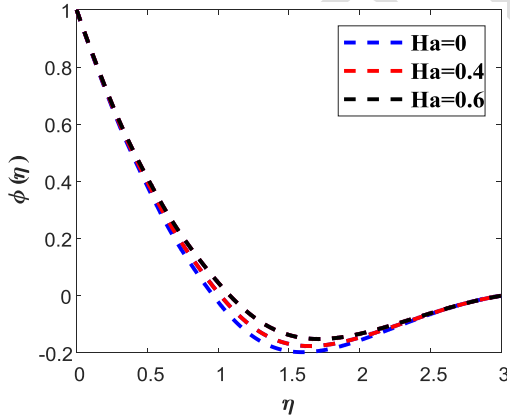

Fig.21. Effect of Hartman number

Pr=6.2,Ld=2.4,B=1, β_1 =0.3 , β_2 =0.4,Gr=0.3,Gr=0.3, L=1.5,Nb=0.8,Ha=0.1,Ec=0.1, α =0.2,N_t=1.2*

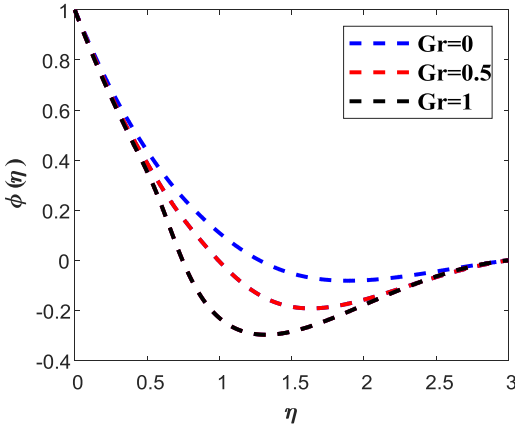

Fig.22. Effect of temperature Grashoff

Pr=2,Ld=2.4,B=1, β_1 =0.3 , β_2 =0.4,Ha=0.1,G=0.3,L=1.5, N_b=0.8,N_t=1.2,Ha=0.1,Ec=0.1, α =0.2

From figs. 17 and 22, Deborah number and temperature Grasshoff thins concentration.

Few nano-particles settle in the high resistive boundary while mass temperature increment lessens the density of nano-particles causing diffusion. Figs.18-21, it is clear that concentration improves with a gain

of solutal stratification, DuFour number, diffusion and Hartman number. At constant density, nano-particles arrange according to size and heat absorbed. The layers pack increasing concentration. The increase in the Dufour number decreases the temperature between the boundary layer and the wall. The temperature gradient results in more heat transfer to the fluid. This lowers internal fluid friction. Similarly, thermophoresis dispenses nano-particles subject to changed density.

4.4. Skin friction and Nusselt number

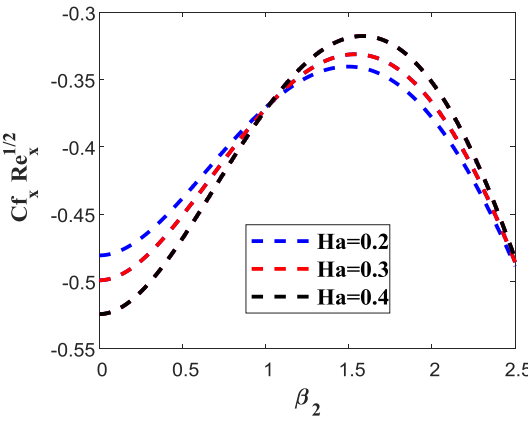

Fig.23. Effects of Hartman and Deborah numbers
Pr=6.2, Ld=2.4, B=1, β_1=0.3, β_2 = 0.8,Gr=0.3,Gr=0.3,N_b=1.6,N_t=1.2, L=1.5,Ec=2.5, α =0.2*

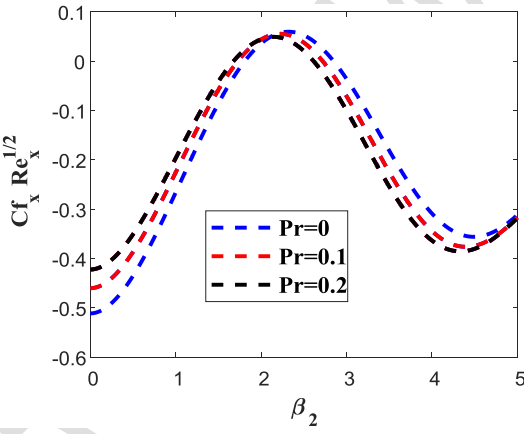

Fig.24. Effects of Prandtl and Deborah numbers
Ld=2.4, B=1, β_1=0.3, β_2 = 0.8,Gr=0.3,Gr=0.3, N_b=1.6,N_t=1.2,L=1.5,Ec=2.5,Ha=0.4, α =0.2*

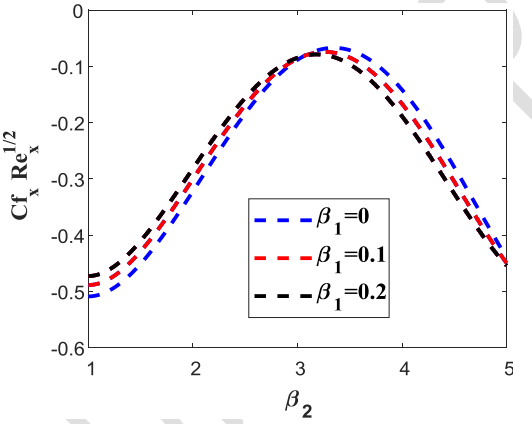

Fig.25. Effects of retardation-relaxation and Deborah
Ld=2.4, B=1,Pr=0.4,Gr=0.3,Gr=0.3,N_b=1.6,N_t=1.2, L=1.5,Ec=2.5,Ha=0.4, α =0.2*

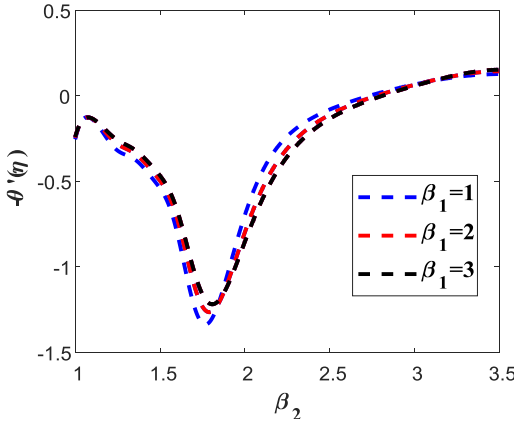

Fig.26.Effects of Retardation-relaxation and Deborah
Ld=2.4, B=1,Pr=0.4,Gr=0.3,G=0.3,N_b=1.6,N_t=1.2, L=1.5,E=2.5,Ha=0.4, α =0.2

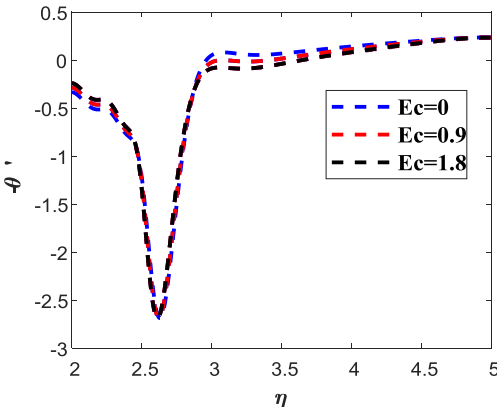

Fig.27. Effect of Eckert number

Pr=6.2,Ld=2.4, B=1, β_2=0.3,β_2=0.8,Gr=1,Gr=0.3, N_b=1.6,N_t=1.2,L=1.5,Ha=0.4, α =0.2*

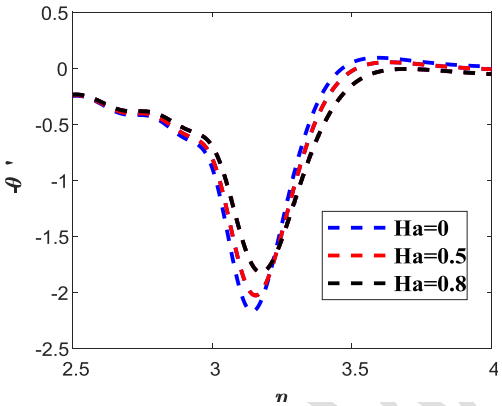

Fig.28.Effect of Hartman number

Pr=6.2,Ld=2.4, Bi=1 , β_1=0.3, β_1==0.8,Ec=0.1 Gr=1,Gr=0.3,N_b=1.6,N_t=1.2,L=1.5, α =0.2*

Fig. 23-25 portray the concurrent effects of increasing Deborah numbers, Hartman numbers, Prandtl number and relaxation-retardation parameter on skin friction. It is noted in fig.23. the skin friction thins at lower numbers of Deborah and Hartman while it thickens at higher numbers; the boundary strata velocity increases. The opposite is observed in fig.24 and 25.

Fig. 26, Deborah number and solutal stratification enhances thermal conductivity by nano-particle conduction at 1 and convection for values greater than 1 . Thermal boundary shrinks at lower numbers. The same effect is observed in figs. 27 and 28.

4.5. Sherwood Number

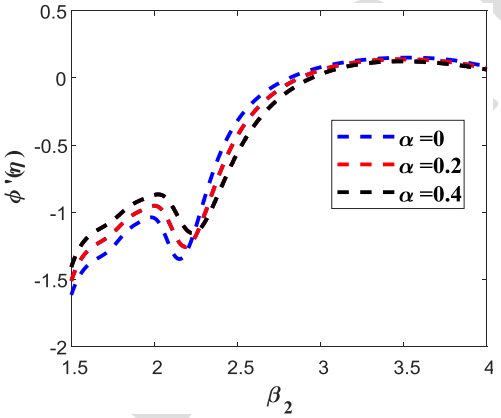

Fig.29. Effects of solutal stratification and Deborah numbers

Pr=6.2,Ld=2.4,B=1,Gr=0.3,Gr=0.3,N_b=1.6,N_t=1.2, L=1.5,Ha=0.1,Ec=2.5, α =0.2*

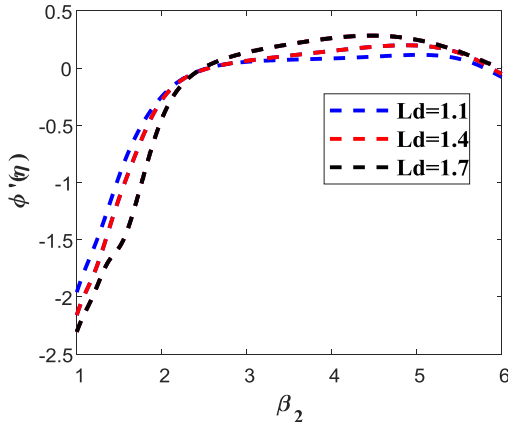

Fig.30.Effect of Dufour-Lewis and Deborah numbers

Pr=6.2, Ld=2.4, B=1, β_1=0.3, Gr=0.3, Gr=0.3, N_b=1.6, N_t=1.2,,L=1.5, Ha=0.1,Ec=2.5, α=0.2*

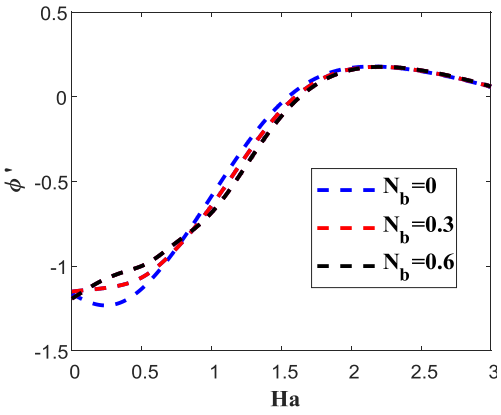

Fig.31. Effects of Hartman number and diffusion
Pr=6.2,Ld=2.4,B=1, 1=0.3, β_2=0.2,Gr=1,Gr*=0.3, N_t=1.2,L=1.5,Ec=0.1, α=0.4

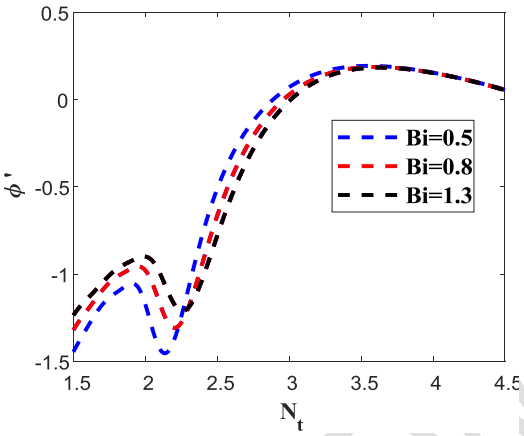

Fig.32.Effects of thermophoresis & Biot number
Pr=6.2,Ld=2.4, β_1=0.3, β_2=0.2,Gr=1,Gr=0.3, Nb=1.3,L=1.5,Ha=0.8,Ec=0.1, α=0.4,Ha=0.8, Nt=1.2*

Figs. 29-30 illustrate the influence of Deborah number, DuFour -Lewis, Biot and Hartman numbers, thermophoresis, diffusion and solutal stratification. Figs.29,31 and 32 discover that a low number of the aforementioned parameters enhance mass transfer. The contrary is seen in fig.30.

5. CONCLUSION

While the increase in Hartman and Prandtl numbers, Relaxation-Retardation and solutal stratification decreased velocity, Deborah number, Mass Grashoff, thermophoresis and mass temperatures increased it.

On the other hand growth in mass-temperature, grasshoff lowered temperature, Hartman number, retardation-relaxation, diffusion and thermophoresis raised it.

Deborah number and temperature Grasshoff thinned concentration, solutal stratification, DuFour number, diffusion and Hartman number improved the concentration. Lower numbers of Deborah and Hartman shrank the skin friction. Large numbers thickened it. Solutal stratification and Deborah number widened the skin friction which increased heat transfer.

Deborah number and solutal stratification shrank thermal boundary at lower numbers. It is discovered that low numbers of Deborah, DuFour -Lewis, Biot and Hartman, thermophoresis, diffusion and solutal stratification enhance mass transfer. The opposite is evidenced by Dufour Lewis and Deborah's numbers.

REFERENCE

1. Zokri, S. M., Arifin, N. S., Kasim, A. R. M., Mohammad, N. F., & Salleh, M. Z. (2018). Boundary layer flow over a moving plate in MHD Jeffrey nanofluid: A revised model. *MATEC Web of Conferences*, *189*, 6–11. https://doi.org/10.1051/matecconf/201818902005
2. Ijaz, M., & Ayub, M. (2019). Thermally stratified flow of Jeffrey fluid with homogeneous-heterogeneous reactions and non-Fourier heat flux model. *Heliyon*, *5*(8). https://doi.org/10.1016/j.heliyon.2019.e02303
3. Murtaza, S., Ali, F., Aamina, Sheikh, N. A., Khan, I., & Nisar, K. S. (2020). Exact analysis of non-linear fractionalized jeffrey fluid. A novel approach of atangana-baleanu fractional model. *Computers, Materials and Continua*, *65*(3), 2033–2047. https://doi.org/10.32604/cmc.2020.011817
4. Rasheed, H. U., Saleem, S., Islam, S., Khan, Z., Khan, W., Firdous, H., & Tariq, A. (2021). Effects of joule heating and viscous dissipation on magnetohydrodynamic boundary layer flow of jeffrey nanofluid over a vertically stretching cylinder. *Coatings*, *11*(3). https://doi.org/10.3390/coatings11030353
5. Agbaje, T. M., & Leach, P. G. L. (2020). Numerical Investigation of Natural Convection Viscoelastic Jeffrey's Nanofluid Flow from a Vertical Permeable Flat Plate with Heat Generation, Thermal Radiation, and Chemical Reaction. *Abstract and Applied Analysis*, *2020*. https://doi.org/10.1155/2020/9816942
6. El-Zahar, E. R., Rashad, A. M., & Seddek, L. F. (2020). Impacts of viscous dissipation and brownian motion on Jeffrey nanofluid flow over an unsteady stretching surface with thermophoresis. *Symmetry*, *12*(9). https://doi.org/10.3390/sym12091450
7. Ur Rasheed, Haroon, Abdou AL-Zubaidi, Saeed Islam, Salman Saleem, Zeeshan Khan, and Waris Khan. 2021. "Effects of Joule Heating and Viscous Dissipation on Magnetohydrodynamic

Boundary Layer Flow of Jeffrey Nanofluid over a Vertically Stretching Cylinder" *Coatings* 11, no. 3: 353. https://doi.org/10.3390/coatings11030353

8. Ge-JiLe, H., Qayyum, S., Shah, F., Khan, M. I., & Khan, S. U. (2021). Slip flow of Jeffrey nanofluid with activation energy and entropy generation applications. *Advances in Mechanical Engineering*, *13*(3), 1–9. https://doi.org/10.1177/16878140211006578
9. Ali, F., Murtaza, S., Khan, I. *et al.* Atangana–Baleanu fractional model for the flow of Jeffrey nanofluid with diffusion-thermo effects: applications in engine oil. *Adv Differ Equ* 2019, 346 (2019). https://doi.org/10.1186/s13662-019-2222-1
10. Srinivasacharya, D., & Shafeeurrahaman, M. (2017). Mixed convection flow of nanofluid in a vertical channel with hall and ion-slip effects. *Frontiers in Heat and Mass Transfer*, *8*(5), 950–959. https://doi.org/10.5098/hmt.8.11
11. Hayat, T., Qayyum, S., & Alsaedi, A. (2017). Mechanisms of nonlinear convective flow of Jeffrey nanofluid due to nonlinear radially stretching sheet with convective conditions and magnetic field. *Results in Physics*, *7*, 2341–2351. https://doi.org/10.1016/j.rinp.2017.06.052
12. Shahzad, F., Sagheer, M., & Hussain, S. (2018). Numerical simulation of magnetohydrodynamic Jeffrey nanofluid flow and heat transfer over a stretching sheet considering Joule heating and viscous dissipation. *AIP Advances*, *8*(6). https://doi.org/10.1063/1.5031447
13. Saleem, S., Rafiq, H., Al-Qahtani, A., El-Aziz, M. A., Malik, M. Y., & Animasaun, I. L. (2019). Magneto Jeffrey Nanofluid Bioconvection over a Rotating Vertical Cone due to Gyrotactic Microorganism. *Mathematical Problems in Engineering*, *2019*. https://doi.org/10.1155/2019/3478037
14. Rasool, G., Shafiq, A., & Durur, H. (2020). Darcy-Forchheimer relation in Magnetohydrodynamic Jeffrey nanofluid flow over stretching surface. *Discrete & Continuous Dynamical Systems - S*, *0*(0), 0. https://doi.org/10.3934/dcdss.2020399